# Tightly Coupled Huygens Element Based Conformal Transmitarray for E-band Airborne Communication Systems

Xuan Wang, Pei-Yuan Qin, *Senior Member, IEEE*, Li-Zhao Song, Ronghong Jin, *Fellow, IEEE* and Y. Jay Guo, *Fellow, IEEE*

***Abstract*—In this paper, a wideband conformal transmitarray employing dual-layer tightly coupled Huygens elements is proposed at E band. The element consists of five pairs of partly overlapped metallic strips with different lengths printed on two sides of a dielectric substrate. It can support tightly coupled Huygens resonances with a high transmission efficiency and a nearly full phase coverage in a wide bandwidth from 71 to 87 GHz. Equivalent circuit models are created to analyze the tightly coupled Huygens element, which has good agreement with that from full-wave simulations. In order to validate the proposed element, a cylindrically conformal transmitarray at 78 GHz is designed, fabricated and measured. Good agreement between the measured and simulated results has been obtained, showing a peak realized gain of 26.6 dBi with an aperture efficiency of 37.2 % from measurement. A measured 3-dB gain bandwidth of 20.4 % is achieved from 71 to 87 GHz, fully covering the E-band spectrum.**

***Index Terms*—Conformal antennas, millimeter-wave, E-band, transmitarrays, tightly coupled Huygens element, wideband.**

## I. Introduction

TRANSMITARRAY antennas have been extensively investigated for space and terrestrial communications because of the ease of achieving high gains and flexible radiation performance [1]-[4]. By employing spatial feed networks that are of low loss and low cost at higher millimeter-wave (mm-wave) bands, transmitarrays are attractive candidates for E-band communication systems to achieve multi-gigabit-per-second wireless point-to-point links [5]-[6]. In this context, substantial efforts have been devoted to different types of transmitarrays, featuring wideband [7]-[9] low radar cross section [10], beam steering [11]-[12] and multi-beam properties [13]-[15]. Recently, conformal transmitarrays, which can follow the mounting platform shapes, have attracted increasing attention due to their excellent aerodynamic performance [16]-[23] for airborne communication systems. Conformal transmitarrays are particularly suitable for unmanned aerial vehicles (UAVs) aided sixth generation (6G) networks to provide a ubiquitous three-dimensional (3-D) coverage.

Considering the reported conformal transmitarrays [16]-[23], one of the most feasible implementation methods is to utilize ultra-thin array elements whose thickness is less than 0.5 mm. This way, the transmitting aperture can be easily bent and attached onto a curved platform. A simple technology is to reduce the thickness of multi-layer elements. Unfortunately, this technology will lead to low antenna efficiencies and narrow bandwidths as the element loss will increase when its thickness is reduced. In [19], a cylindrically conformal transmitarray employing triple-layer slot elements was developed with a realized gain of 19.6 dBi, an aperture efficiency of 25.1 % and a 3-dB gain bandwidth of 6.7%. A potential solution to improve the antenna efficiency is to employ Huygens metasurfaces as they can achieve nearly total transmission and zero reflection with thin profiles. In [20], an efficient conformal transmitarray was developed based on dual-layer ultra-thin Huygens elements with a peak gain of 20.6 dBi, a 47% aperture efficiency and a 3-dB gain bandwidth of 3.7%. It should be noted that although the efficiency of the conformal transmitarray in [20] has been significantly improved compared to that in [19], its 3-dB gain bandwidth is very narrow. This is because a Huygens resonance has a narrow band property. As a result, they are not suitable for most practical E-band applications as it cannot cover the entire E-band. This disadvantage has also been found in some planar Huygens element based transmitarrays [24]-[27]. In [24] and [25], the reported designs have a 3-dB gain bandwidth of less than 5.0 %. In [26], a dual-layer Huygens element is presented at 60 GHz with a 1.5-dB gain bandwidth from 58 GHz to 62 GHz (6.7 %). In [27], a 1-bit planar beam scanning transmitarray is developed using a reconfigurable dual-layer strip-line Huygens element. The 180° phase difference between the two states of the Huygens element is achieved in a narrow bandwidth, resulting in beam scanning in a bandwidth of about 5.4 % and a 3-dB gain bandwidth of 9.4 % for the boresight radiation. By

This work was supported by the Australia Research Council Discovery Program under Grant DP 220101158 and DP230101955.

X. Wang is with the Department of Electronic Engineering, Shanghai Jiao Tong University, Shanghai 200240, China, and was with the Global Big Data Technologies Centre, University of Technology Sydney, Ultimo, NSW 2007, Australia.

P.-Y. Qin and Y. J. Guo are with the Global Big Data Technologies Centre, University of Technology Sydney, Ultimo, NSW 2007, Australia (e-mail: pyqin1983@hotmail.com).

L.-Z. Song is with the Manufacturing, Commonwealth Scientific and Industrial Research Organization (CSIRO), Lindfield, NSW, 2070, Australia.

R. Jin is with the Department of Electronic Engineering, Shanghai Jiao Tong University, Shanghai 200240, China.

using a dual-layer Huygens element consisting of a pair of antisymmetric conducting semicircle arcs, a planar transmitarray in [28] can achieve a wide 3-dB gain bandwidth of 15.7 % at 26.2 GHz with a gain of 30.7 dBi. However, this reported bandwidth cannot fully cover E-band spectrum.

There are some methods reported to enhance the bandwidth of planar and conformal transmitarrays [29]-[33]. In [29], a triple-layer frequency-selective surface (FSS) element is proposed for a wideband planar transmitarray, showing a 1-dB gain bandwidth of 16.8 %. The element is printed on three substrates separated by two air gaps. In [30], a wideband planar transmitarray with a 1-dB gain bandwidth of 16 % is developed by employing two identical triple-layer FSSs separated by an air gap. In [31], a wideband dual-circularly polarized transmitarray employing a 5-layer element with two metallic vias is proposed, showing a 2-dB gain bandwidth of 12 %. However, it should be noted that all these techniques employ multi-layer elements with air gaps or metallic vias, which are not suitable for conformal transmitarrays as it is difficult for these structures to sustain the bending process. In [21], an ultrawideband conformal transmitarray is presented using a three-dimensional (3D) element consisting of a planar slot-bowtie radiator and meander slot-lines perpendicular to the slot-bowtie surface. A potential limitation of this work is that each row of array elements is fabricated on discrete printed circuit boards and the boards are stacked on top of each other. This complex design makes it very challenging to assemble a large array and may introduce large fabrication errors in E-band compared with circuits printed in one piece. Furthermore, the ultrawideband is achieved in terms of stable radiation patterns rather than a wide 3-dB gain bandwidth.

In this paper, a wideband conformal transmitarray employing dual-layer tightly coupled Huygens elements at E-band is developed. The element consists of five pairs of partly overlapped metallic strips with different lengths. These five pairs of strips are placed closely to each other, which can provide tightly coupled Huygens resonances with nearly total transmission and full transmission phase coverages in a wide bandwidth. To validate the design concept, a cylindrically conformal transmitarray at 78 GHz is designed, fabricated and measured. Good agreement between measurement and simulation has been achieved, showing a peak measured realized gain of 26.6 dBi with an aperture efficiency of 37.2 %. The measured 3-dB gain bandwidth is 20.4 % from 71 to 87 GHz. Compared with other conformal transmitarrays [19]-[20] or some planar transmitarrays using dual-layer elements [25]-[28] without metallic vias and air gaps, the developed tightly coupled multiple Huygens resonances based transmitarray can achieve a much wider gain bandwidth.

The rest part of the paper is organized as follows. Section II describes the configuration, equivalent circuit models and the frequency responses of the dual-layer tightly coupled Huygens element. In Section III, a cylindrically conformal transmitarray employing the proposed elements is shown. The numerical and experimental results of the conformal transmitarray antenna are discussed in Section IV. The paper concludes in Section V.

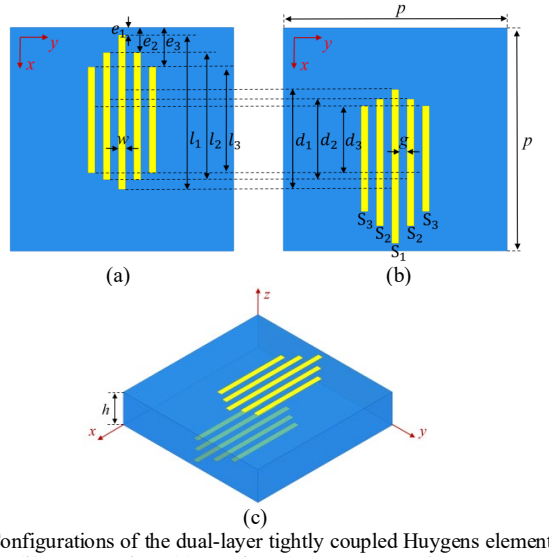


Fig. 1. Configurations of the dual-layer tightly coupled Huygens element. (a) Top view. (b) Bottom view. (c) 3D view. ($p$ = 2.401 mm, $l_1$ = 1.655 mm, $l_2$ = 1.366 mm, $l_3$ = 1.138 mm, $d_1$ = 1.073 mm, $d_2$ = 0.868 mm, $d_3$ = 0.723 mm, $e_{1,2,3}$ = ($p$+$d_{1,2,3}$)/2-$l_{1,2,3}$, $w$ = 0.075 mm, $g$ = 0.088 mm and $h$ = 0.508 mm.)

## II. Dual-Layer Tightly Coupled Huygens Element

Theoretically, a Huygens element consists of a pair of orthogonally induced electric and magnetic currents which are in phase. The balanced condition between electric and magnetic responses can result in a total transmission and zero reflection, which can support a high-efficiency transmitarray design. Unfortunately, the strong resonance of a Huygens element can lead to a very narrow bandwidth, which is not suitable for many wireless communication systems.

To increase the bandwidth, a dual-layer tightly coupled Huygens element is proposed, as shown in Fig. 1. It consists of five pairs of partly overlapped metallic strips. The middle pair of strips is marked as $S_1$, the two pairs of strips next to it are marked as $S_2$, and the two pairs at the edges are marked as $S_3$. The five pairs are symmetric along $x$-axis with different lengths fabricated on one dielectric substrate. The dielectric substrate employed is Rogers RT/duroid 5880 (relative permittivity of 2.2, dielectric loss tangent of 0.0009 and thickness $h$ of 0.508 mm). The bottom metallic strips shown in Fig. 1 (b) can be obtained by rotating the top metallic strips shown in Fig. 1 (a) by 180° along $z$-axis.

For an $x$-polarized incidence wave, the tightly coupled Huygens element shown in Fig. 1 can be considered as five dual-layer Huygens resonances in parallel. In order to analyze the operating mechanism of the proposed tightly coupled Huygens element, we start to investigate a single pair of Huygens element, e.g., the middle pair of strips $S_1$.

Based on the method discussed in [26], we present an equivalent circuit model to describe the working principle of the Huygens element with one pair of strips, as shown in Fig. 2 (a). Under $x$-polarized incidence waves, electric currents on the metallic strip of the top or bottom layer are induced, which are represented by an inductance, $L$. A series capacitance $C_1$ exists between the metallic strips of the top or bottom layer of the two neighboring elements along $x$-axis. The dielectric substrate is represented by a transmission line with a characteristic

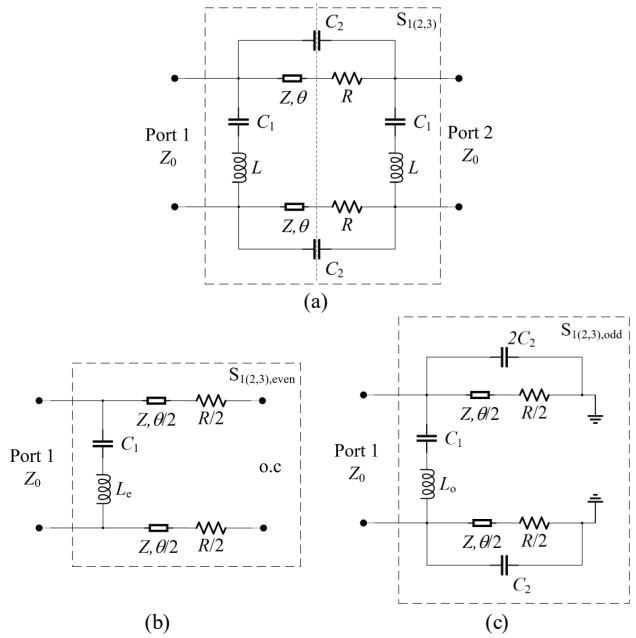


Fig. 2. (a) Equivalent circuit model, (b) even mode decomposed circuit and (c) odd mode decomposed circuit of the Huygens element with only a pair of strips, e.g., $S_1$, $S_2$ or $S_3$.

impedance of $Z$ with an electrical length of $\theta$ and a resistor of $R$. The resistor represents the dielectric losses leading to unavoidable transmission losses in the Huygens element at E-band. A coupling capacitance also exists between the two metallic strips of top and bottom layers, represented by a capacitance $C_2$. The equivalent circuit shown in Fig. 2 (a) can be further split to emphasize longitudinal symmetries of the structure. The longitudinal symmetry allows an even-odd mode decomposition of the structure. The even and odd mode decomposed circuits are shown in Figs. 2 (b) and 2 (c), respectively. In the even mode, the coupling capacitance $C_2$ has no contribution due to open circuit termination at the longitudinal symmetry plane, as shown in Fig. 2 (b). This even mode can provide an electric response for the Huygens resonance. As shown in Fig. 2 (c), in the odd mode, the coupling capacitance $C_2$ leads to the displacement currents between the two metallic strips of the top and bottom layers. These displacement currents with the induced currents on the top and bottom layers can form a current loop, which can be equivalent to a magnetic response for the Huygens resonance [34]. Moreover, the transmission and reflection coefficients of the Huygens element can be obtained using the superposition of the even and odd modes [26]:

$$S_{21} = \left(\frac{S_{11,even} + S_{11,odd}}{2}\right) \quad (1)$$

$$S_{11} = \left(\frac{S_{11,even} - S_{11,odd}}{2}\right) \quad (2)$$

In order to determine the values of the equivalent circuit components, the Huygens element with only a pair of strips $S_1$ is firstly simulated using master/slave boundary conditions and Floquet ports by 3D EM simulation software HFSS. As seen from Fig. 3, the transmission loss of the Huygens element with only a pair of strips $S_1$ is less than 2.7 dB and transmission phase coverage is about 262° from 65 to 90 GHz. Then, based on equations (1) and (2), by using numerical optimizations to

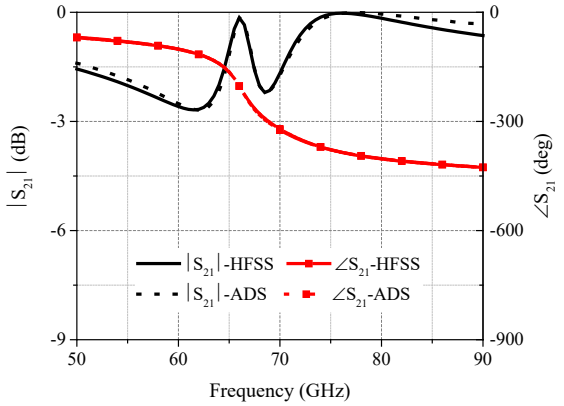


Fig. 3. Transmission coefficients of the Huygens element with only a pair of strips $S_1$.

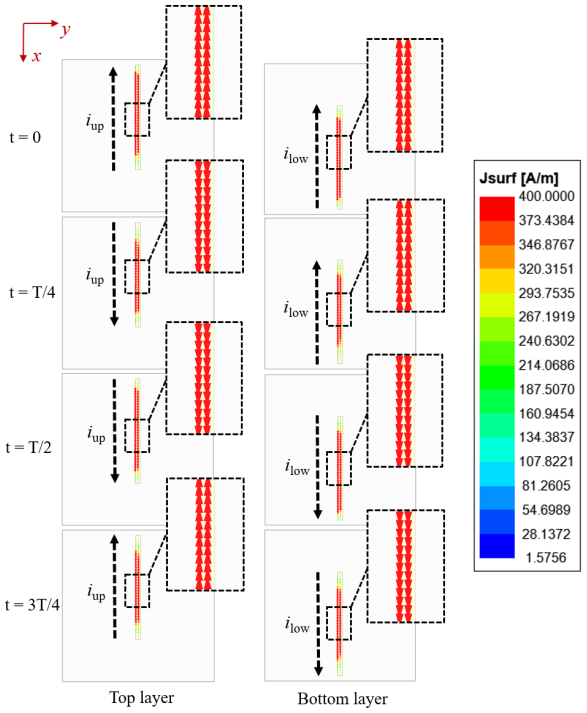


Fig. 4. Induced surface currents on top and bottom layers of the Huygens element with only a pair of strips $S_1$ in a time period T.

match the full-wave response of the element in Fig. 3, the values of the circuit components can be decided. The values of the parameters of the Huygens element with only a pair of strips $S_1$ are as follows: $L_e = 3.26$ nH, $L_o = 2.73$ nH, $C_1 = 1.89$ fF. $C_2 = 0.55$ fF, $Z_0 = 377$ Ω, $Z = 254$ Ω, $\theta = 60.58°$ and $R = 1.77$ Ω.

When an x-polarized wave impinges on the Huygens element with only a pair of strips $S_1$, the induced surface currents on the two metallic layers at 78 GHz are shown in Fig. 4. The currents on top and bottom layers are represented as $i_{up}$ and $i_{low}$, respectively. As shown in Fig. 4, the directions of $i_{up}$ and $i_{low}$ are the same in the first and third quarters of a time period T, providing an electric response along $x$-axis. In the second and fourth quarters of T, the directions of $i_{up}$ and $i_{low}$ are opposite, providing a current loop which is equivalent to a magnetic response with a time delay of T/4. Thus, the induced electric and magnetic currents are orthogonal and they appear simultaneously. This can excite a Huygens resonance in the

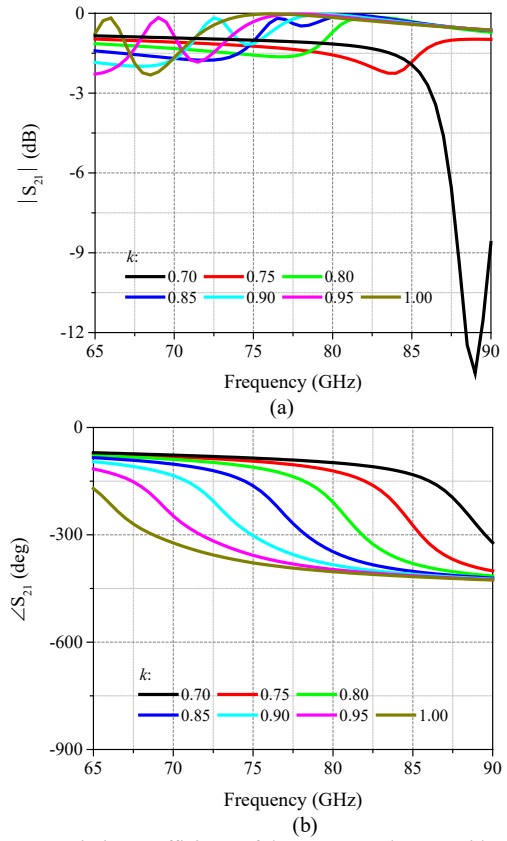


Fig. 5. Transmission coefficients of the Huygens element with only a pair of strips $S_1$ and different values of scale factor $k$. (a) Magnitudes. (b) Phases.

element. The length of the metallic strip, $l_1$, along $x$-axis controls the Huygens resonant frequency and the length of the overlapped metallic strip, $d_1$, provide a fine tuning to achieve the balanced condition of the Huygens resonance.

Changing the parameters $l_1$ and $d_1$ by a scale factor $k$ from 0.70 to 1.00, the transmission phase can be tuned. The transmission coefficients versus frequencies from 65 to 90 GHz of the Huygens element with only a pair of strips $S_1$ and different values of $k$ are shown in Fig. 5. It can be seen that the transmission losses of the element are larger than 3 dB above 86.5 GHz when $k$ is 0.70. Furthermore, the transmission phase ranges are less than 259° above 86.5 GHz. These insufficient phase coverages will lead to phase errors and reduce the bandwidth of the transmitarray. Especially, it will have more impact on higher frequencies as larger phase compensation values are needed. Thus, the Huygens element with a single pair of strips is not suitable for a wideband transmitarray design.

To achieve less than 3 dB transmission losses and a larger phase tuning range (especially at higher frequencies of E-band), the tightly coupled Huygens element shown in Fig. 1 is proposed. For $x$-polarized incidence waves, the dual-layer tightly coupled Huygens element can be seen as five dual-layer Huygens resonances in parallel. The equivalent circuit model of the proposed element is composed of five equivalent circuits of dual-layer Huygens resonance (one pair of strips) in parallel with coupling capacitances, $C_{S2,even}$, $C_{S3,even}$, $C_{S2,odd}$ and $C_{S2,odd}$, representing the tightly coupling effects among the Huygens

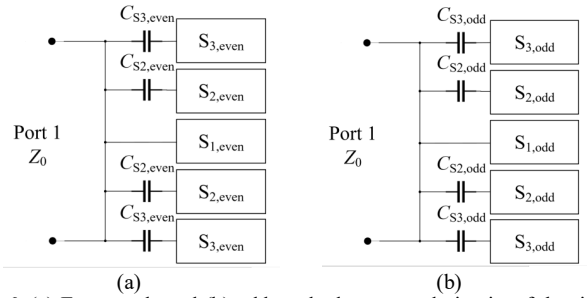


Fig. 6. (a) Even mode and (b) odd mode decomposed circuits of the tightly coupled Huygens element consisting of five pairs of strips.

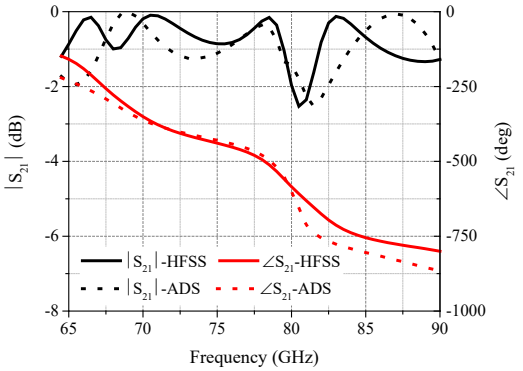


Fig. 7. Transmission coefficients of the tightly coupled Huygens element.

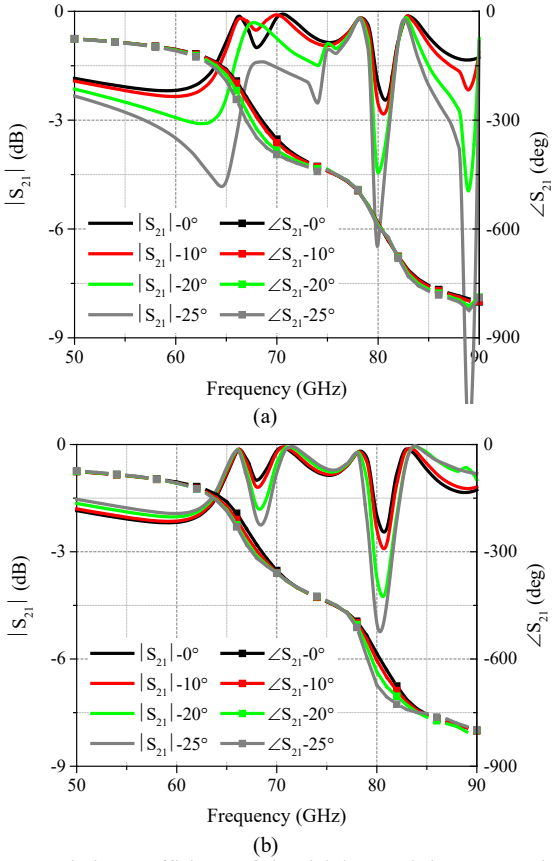


Fig. 8. Transmission coefficients of the tightly coupled Huygens element under the oblique incidence waves with different angles. (a) TE waves. (b) TM waves.

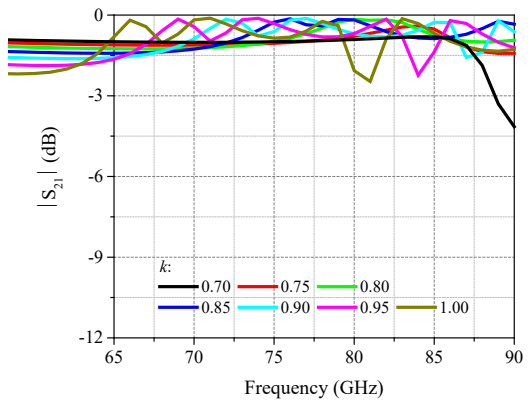


(a)

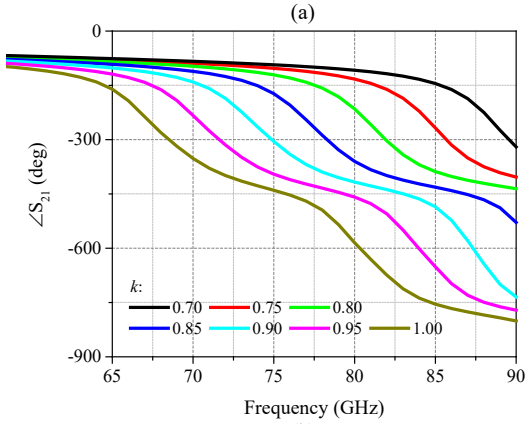


(b)

Fig. 9. Transmission coefficients of the tightly coupled Huygens element with different values of scale factor *k*. (a) Magnitudes. (b) Phases.

resonances [35] as shown in Fig. 6. $S_{1,even}$, $S_{2,even}$ and $S_{3,even}$ denote the even mode decomposed circuits of the Huygens element with a pair of strips $S_1$, $S_2$ or $S_3$, respectively. $S_{1,odd}$, $S_{2,odd}$ and $S_{3,odd}$ denote the odd mode decomposed circuits of the Huygens element with a pair of strips $S_1$, $S_2$ or $S_3$, respectively. The equivalent circuit models of the even and odd mode decomposed circuits of the Huygens element with strips $S_1$, $S_2$ or $S_3$ have the same topological circuits shown in Fig. 2. The values of the circuit parameters of $S_{1,even}$ and $S_{1,odd}$ are provided previously. The values of the circuit parameters of $S_{2,even}$ and $S_{2,odd}$ are as follows: $L_e$ = 4.82 nH, $L_o$ = 2.91 nH, $C_1$ = 1.11 fF. $C_2$ = 0.57 fF, $Z_0$ = 377 Ω, $Z$ = 254 Ω, $\theta$ = 60.58° and $R$ = 2.23 Ω. The values of the circuit parameters of $S_{3,even}$ and $S_{3,odd}$ are as follows: $L_e$ = 4.82 nH, $L_o$ = 3.64 nH, $C_1$ = 0.68 fF. $C_2$ = 0.26 fF, $Z_0$ = 377 Ω, $Z$ = 254 Ω, $\theta$ = 60.58° and $R$ = 2.23 Ω. Moreover, the coupling capacitances among strips $S_1$, $S_2$ and $S_3$ are $C_{S2,even}$ = 2.99 fF and $C_{S3,even}$ = 0.10 fF in the even mode; $C_{S2,odd}$ = 0.60 fF and $C_{S3,odd}$ = 3.38 fF in the odd mode.

The transmission magnitude and phase of the dual-layer tightly coupled Huygens element are obtained using both 3D simulation and circuit analysis. As shown in Fig. 7, good agreement between these two methods is obtained. It is noticed that the transmission loss is less than 2.5 dB and the phase variation range is 641° from 65 to 90 GHz for the tightly coupled Huygens element. Compared to the Huygens element with only one pair of strips, multiple Huygens resonances are realized in the tightly coupled Huygens element. This way, the transmission loss is reduced and the transmission phase

TABLE I
TRANSMISSION LOSSES AND PHASE COVERAGES OF THE DUAL-LAYER TIGHTLY COUPLED HUYGENS ELEMENT AT DIFFERENT FREQUENCIES

| Frequency | 71 GHz | 73 GHz | 75 GHz |
|---|---|---|---|
| Transmission loss | 1.3 dB | 1.2 dB | 1.1 dB |
| Phase coverage | 297° | 328° | 349° |
| Frequency | 77 GHz | 79 GHz | 81 GHz |
| Transmission loss | 1.1 dB | 1.0 dB | 2.4 dB |
| Phase coverage | 374° | 432° | 521° |
| Frequency | 83 GHz | 85 GHz | 87 GHz |
| Transmission loss | 2.2 dB | 1.8 dB | 1.3 dB |
| Phase coverage | 592° | 617° | 601° |

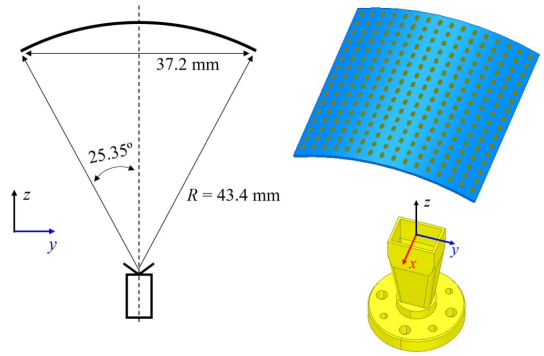


(a) (b)

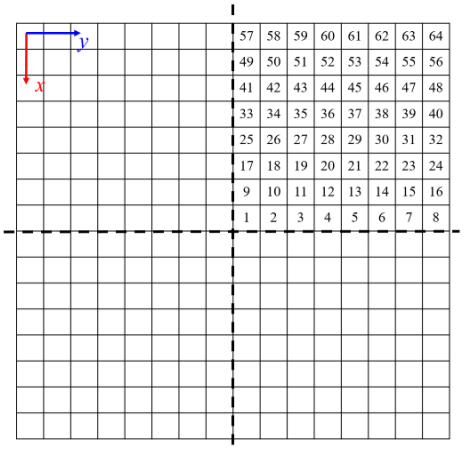


(c)

Fig. 10. Cylindrically conformal Transmitarray. (a) Sketch of front view; (b) 3D structure. (c) Unfolded transmitting surface.

coverage is increased greatly. The transmission magnitudes and phases of the proposed element under the oblique incidence TE and TM waves with different angles from 0° to 25° are shown in Figs. 8 (a) and 8 (b), respectively. It is seen that the transmission losses remain reasonably stable with different incident angles. Only at a few frequencies they are larger than 3 dB when the incidence angle is around 25°. But this will only affect a small number of elements at the edge of the transmitting aperture, which may not reduce the antenna gain significantly as shown in the simulated and measured array results in the Section IV. The transmission phases are very stable for different incidence angles, which is beneficial to a wideband high-efficiency transmitarray.

Changing the parameters $l_1$, $l_2$, $l_3$, $d_1$, $d_2$ and $d_3$ by a scale factor $k$ from 0.70 to 1.00, the simulated transmission

TABLE II
TRANSMISSION LOSSES AND PHASES OF THE TIGHTLY COUPLED HUYGENS ELEMENT WITH DIFFERENT VALUES OF SCALE FACTOR $K$ AT 78 GHZ

| No. | $k$ | Tran. loss (dB) | Tran. phase (deg) | No. | $k$ | Tran. loss (dB) | Tran. phase (deg) |
|---|---|---|---|---|---|---|---|
| 1 | 0.900 | 0.4 | -398 | 33 | 0.836 | 0.4 | -275 |
| 2 | 0.889 | 0.2 | -386 | 34 | 0.832 | 0.4 | -263 |
| 3 | 0.872 | 0.1 | -361 | 35 | 0.824 | 0.3 | -238 |
| 4 | 0.854 | 0.3 | -325 | 36 | 0.811 | 0.2 | -199 |
| 5 | 0.836 | 0.4 | -275 | 37 | 0.785 | 0.7 | -150 |
| 6 | 0.816 | 0.2 | -213 | 38 | 0.954 | 0.8 | -447 |
| 7 | 0.774 | 0.9 | -138 | 39 | 0.880 | 0.1 | -374 |
| 8 | 0.914 | 0.5 | -412 | 40 | 0.840 | 0.5 | -287 |
| 9 | 0.889 | 0.2 | -386 | 41 | 0.816 | 0.2 | -213 |
| 10 | 0.880 | 0.1 | -374 | 42 | 0.812 | 0.2 | -202 |
| 11 | 0.865 | 0.1 | -349 | 43 | 0.802 | 0.3 | -178 |
| 12 | 0.849 | 0.4 | -312 | 44 | 0.775 | 0.9 | -139 |
| 13 | 0.832 | 0.4 | -263 | 45 | 0.956 | 0.8 | -449 |
| 14 | 0.811 | 0.2 | -199 | 46 | 0.890 | 0.2 | -387 |
| 15 | 0.758 | 1.0 | -125 | 47 | 0.849 | 0.4 | -312 |
| 16 | 0.900 | 0.4 | -398 | 48 | 0.821 | 0.2 | -228 |
| 17 | 0.872 | 0.1 | -361 | 49 | 0.779 | 0.8 | -142 |
| 18 | 0.865 | 0.1 | -349 | 50 | 0.765 | 0.9 | -130 |
| 19 | 0.854 | 0.3 | -325 | 51 | 0.970 | 0.6 | -465 |
| 20 | 0.840 | 0.5 | -287 | 52 | 0.932 | 0.7 | -427 |
| 21 | 0.824 | 0.3 | -238 | 53 | 0.883 | 0.2 | -378 |
| 22 | 0.801 | 0.3 | -176 | 54 | 0.850 | 0.3 | -315 |
| 23 | 0.966 | 0.7 | -460 | 55 | 0.825 | 0.3 | -241 |
| 24 | 0.880 | 0.1 | -374 | 56 | 0.789 | 0.6 | -155 |
| 25 | 0.854 | 0.3 | -325 | 57 | 0.923 | 0.6 | -419 |
| 26 | 0.849 | 0.4 | -312 | 58 | 0.910 | 0.5 | -408 |
| 27 | 0.840 | 0.5 | -287 | 59 | 0.889 | 0.2 | -386 |
| 28 | 0.828 | 0.3 | -251 | 60 | 0.863 | 0.2 | -345 |
| 29 | 0.811 | 0.2 | -199 | 61 | 0.843 | 0.4 | -296 |
| 30 | 0.773 | 0.9 | -137 | 62 | 0.823 | 0.2 | -234 |
| 31 | 0.925 | 0.7 | -421 | 63 | 0.792 | 0.6 | -159 |
| 32 | 0.859 | 0.2 | -337 | 64 | 0.939 | 0.8 | -433 |

coefficients versus frequencies of the proposed tightly coupled element from 65 to 90 GHz are shown in Fig. 9. The maximum transmission losses and phase coverages of the elements at different frequencies are summarized in Table I. From 71 GHz to 87 GHz, the maximum transmission loss is less than 2.4 dB. The phase coverage is between 297° and 617° from 71 to 87 GHz. It should be noted that the phase tuning range of the tightly coupled Huygens element is significantly enlarged at higher frequencies of E-band, compared to the element with a single pair of strips. For example, at 87 GHz, it is 601° and 250° for the tightly coupled Huygens element and the element with single Huygens resonance, respectively. This is particularly useful for a wideband transmitarray. At lower band, an about 300° phase coverage is realized, which is sufficient for a transmitarray design with an acceptable realized gain drop as shown in the simulated and measured array results in the Section IV. In conclusion, with different values of the scale factor $k$, the proposed tightly coupled Huygens element provides over 300° continuous phase coverages and the transmission loss is less than 2.4 dB from 71 to 87 GHz, corresponding to a bandwidth of 20.2 %.

## III. WIDEBAND CONFORMAL TRANSMITARRAY ANTENNA PROTOTYPE

The transmitarray aperture was fabricated using standard PCB technology. Then, the aperture was bent onto a 3D printed

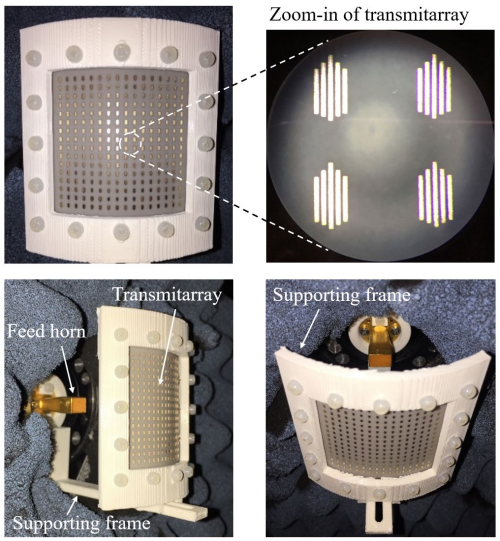


Fig. 11. Photographs of the fabricated wideband conformal transmitarray antenna.

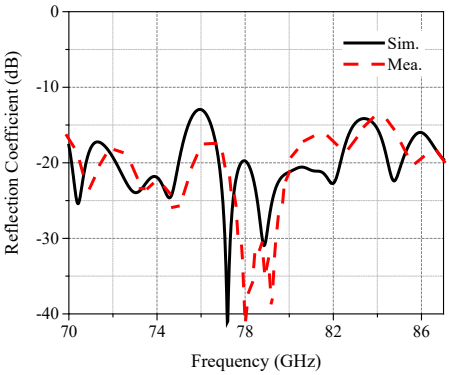


Fig. 12. Measured and simulated reflection coefficients of the wideband conformal transmitarray antenna.

cylindrical surface. To ensure the aperture is bendable, the thickness of the aperture needs be very thin. By using this implementation method, the proposed tightly coupled structure is limited to antennas operating at high frequency bands. However, by using the direct ink printing technology or laser technology from LPKF [36], for instance, metal can be printed directly on a curved substrate. This way, the thickness of the substrate may not be very thin, and the proposed design method can be applied to lower frequency bands. To verify the feasibility of the proposed dual-layer tightly coupled Huygens element, a cylindrically conformal transmitarray is designed with 16×16=256 elements, as shown in Figs. 10 (a) and 10 (b). The cross-section size of the transmitting aperture is 37.2 mm × 38.4 mm ($9.7\lambda \times 10\lambda$ at 78 GHz). A standard gain horn LB-12-15 from A-INFO is located at the focal point. The focal length is 43.4 mm. The realized gain of LB-12-15 from the data sheet is 15.6 dB at 78 GHz. The phase compensations of the transmitarray are achieved by varying the scale factor $k$ of each element on the aperture. Since the conformal transmitarray is symmetrical along both $x$- and $y$-axes, the scale factors $k$ and simulated transmission coefficients of the elements on a quarter of the whole conformal transmitarray at 78 GHz are shown in Fig. 10 (c) and Table II, respectively. It can be seen that the

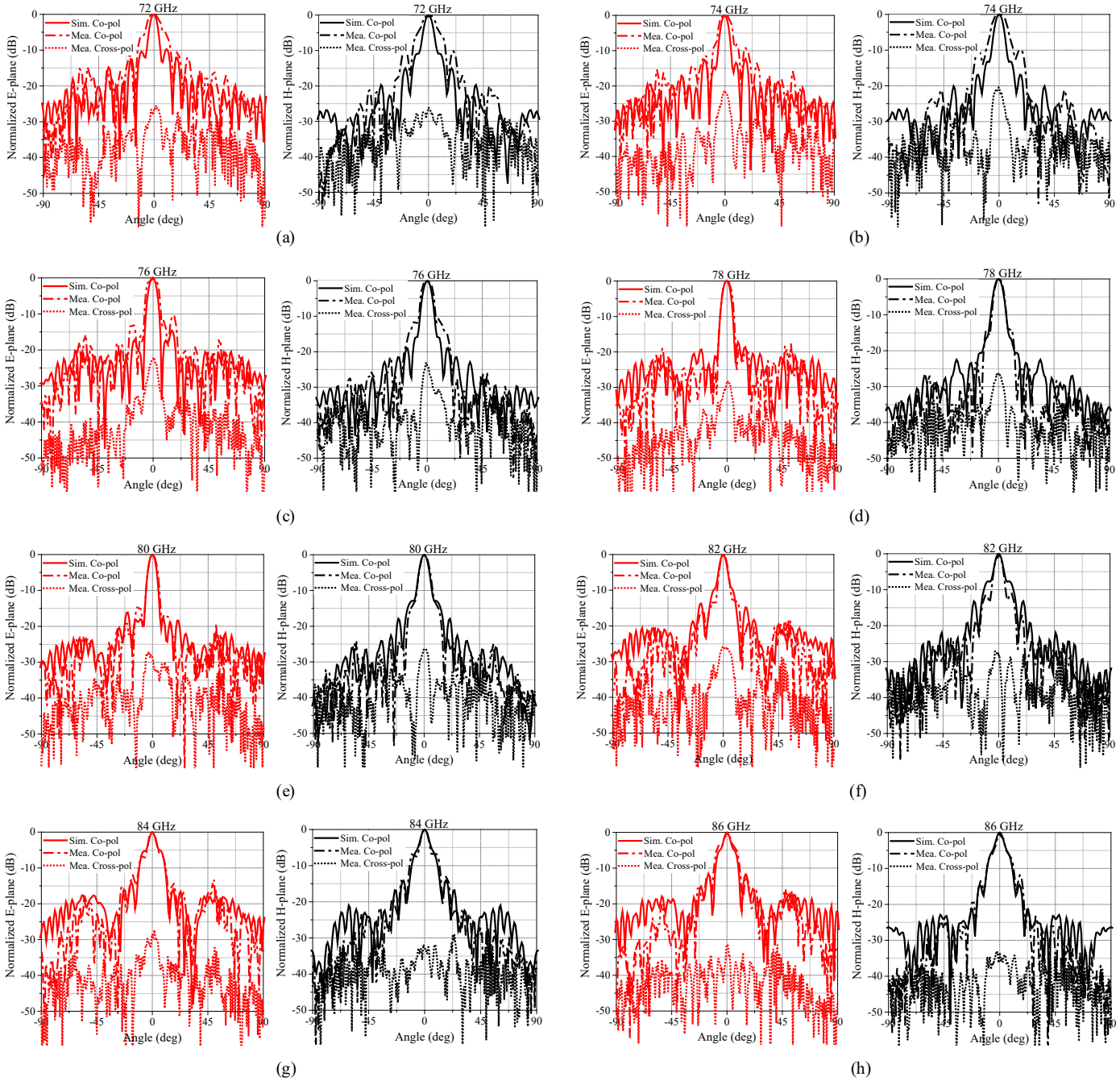


Fig. 13. Measured and simulated patterns of the wideband conformal transmitarray antenna in E-plane (red) and H-plane (black) at different frequencies. (a) 72 GHz. (b) 74 GHz. (c) 76 GHz. (d) 78 GHz. (e) 80 GHz. (f) 82 GHz. (g) 84 GHz. (h) 86 GHz.

transmission losses of all elements on the conformal transmitarray are less than 0.9 dB which can facilitate a high-efficiency transmitarray design. Besides, continuous phase compensations are achieved.

## IV. Numerical And Experiment Results Of The Wideband Conformal Transmitarray Antenna

The fabricated prototype of the wideband conformal transmitarray antenna is shown in Fig. 11. The input reflection coefficients $|S_{11}|$ of the transmitarray antenna are measured using a Keysight Vector Network Analyzer (VNA) N5225A with a 60-90 GHz VNA extender. As shown in Fig. 12, the measured and simulated input reflection coefficients of the antenna are below -10 dB from 70 GHz to 87 GHz. We measured the far-field radiation pattens of the transmitarray in a compact range antenna measurement system at University of Technology Sydney, Australia. The measured and simulated normalized radiation patterns along E and H planes at different frequencies are plotted in Fig. 13. It can be seen that the radiation patterns remain stable across the band and all side lobe levels (SLLs) are less than -10 dB. The measured and simulated realized gains and aperture efficiencies of the conformal transmitarray antenna versus frequencies from 70 to

TABLE III
COMPARISONS BETWEEN REPORTED TRANSMITARRAY ANTENNAS

| Ref. | Configuration | Thickness | Conformality | Frequency | Gain | Aperture eff. | 3/1.5-dB gain bandwidth |
|---|---|---|---|---|---|---|---|
| [19] | 3-layer | $0.040\lambda_0$ | Conformal | 25.0 GHz | 19.6 dBi | 25.1 % | 6.7 % / 4.3 % |
| [20] | 2-layer | $0.017\lambda_0$ | Conformal | 10.0 GHz | 20.6 dBi | 47.0 % | 3.7 % / 2.3 % |
| [25] | 2-layer | $0.045\lambda_0$ | Planar | 9.3 GHz | 19.6 dBi | 27.8 % | 3.2 % / Non shown |
| [26] | 2-layer | $0.104\lambda_0$ | Planar | 61.5 GHz | 31.0 dBi | N/A | Non shown / 6.7 % |
| [27] | 2-layer | $0.135\lambda_0$ | Planar | 12.8 GHz | 18.4 dBi | 20.2 % | 9.4 % / 5.6 % |
| [28] | 2-layer | $0.131\lambda_0$ | Planar | 26.2 GHz | 30.7 dBi | 42.2 % | 15.7 % / 8.3 % |
| **This work** | **2-layer** | **$0.133\lambda_0$** | **Conformal** | **78.5 GHz** | **26.6 dBi** | **37.2 %** | **20.4 % / 15.2 %** |

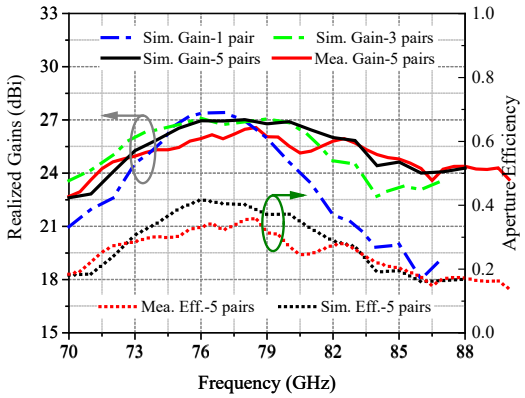


Fig. 14. Measured and simulated realized gains and aperture efficiencies of the wideband conformal transmitarray antenna versus frequencies.

88 GHz are shown in Fig. 14. The measured results show a peak realized gain of 26.6 dBi with an aperture efficiency of 37.2 % at 78.5 GHz. The measured 3-dB gain bandwidth is 20.4 % from 71 to 87 GHz, fully covering the E-band spectrum from 71 to 86 GHz. It should be noted that the 3-dB gain bandwidth increases with the number of the strip pairs in the transmitarray element. The simulated realized gains of the transmitarrays employing the elements with 1 and 3 pairs of strips are also shown in Fig. 14. The simulated 3-dB gain bandwidths are 9.0 % from 73 to 80 GHz and 15.4 % from 71 to 83 GHz, respectively. Thus, the tightly coupled Huygens element can significantly improve the gain bandwidth of the transmitarray.

A comparison among this work and other reported planar or conformal transmitarrays is presented in Table III. It can be seen that the proposed conformal design is the only one working at E band and it can provide a much larger 3/1.5-dB gain bandwidth compared with other conformal transmitarrays and many planar ones. Please be noted that the thicknesses of the elements in [27]-[28] and this work are all about $0.13\lambda_0$ ($\lambda_0$ is the wavelength in the free space). There are some reported 2-layer elements with smaller thickness [20], [25], but their 3-dB bandwidths are less than 7 %. Based on this work, a dual-polarized wideband tightly coupled dual-layer Huygens surface can also be developed, but two challenges must be addressed. The first one is to locate two sets of tightly coupled Huygens strips on the element with very small mutual coupling between them. The second one is to achieve sufficient phase variation range and low transmission losses for both sets of tightly coupled Huygens strips with different polarizations. This is the focus of our on-going research.

## V. CONCLUSION

A wideband conformal transmitarray employing dual-layer tightly coupled Huygens elements is proposed for E-band communications in the paper. The element consists of five pairs of partly overlapped metallic strips with different lengths printed on two sides of a dielectric substrate. It can provide tightly coupled Huygens resonances with nearly total transmission and full transmission phase coverage in a wide bandwidth. To validate the design concept, a cylindrically conformal transmitarray at 78 GHz is designed, fabricated and measured. Good agreement between the measured and simulated results is found, showing a peak measured realized gain of 26.6 dBi and an aperture efficiency of 37.2 % at 78.5 GHz. The measured 3-dB gain bandwidth is 20.4 % from 71 to 87 GHz, fully covering the E-band spectrum from 71 to 86 GHz.

## REFERENCES


[1] Q. Luo, S. Gao, W. Liu, and C. Gu, *Low-cost smart antennas*. Hoboken, NJ, USA: Wiley, 2019.

[2] A. H. Abdelrahman, F. Yang, A. Z. Elsherbeni, P. Nayeri, and C. A. Balanis, *Analysis and design of transmitarray antennas*. San Francisco, CA, USA: Morgan & Claypool, 2017.

[3] S. Gaber, S. H. Zainud-Deen and H. A. E. Malhat, "Analysis and design of reflectarrays/transmitarrays antennas," *LAP LAMBERT Academic Publ,* 2014.

[4] L. Dussopt, "Transmitarray antennas", A. Boriskin and R. Sauleau (eds), *Aperture antennas for millimeter and sub-millimeter wave applicatons*, Springer 2018.

[5] P. Rost, et al., "Mobile network architecture evolution toward 5G," *IEEE Commun. Mag.*, vol. 54, no. 5, May 2016, pp. 84-91.

[6] P.-Y. Qin, L.-Z. Song and Y. J. Guo, "Conformal transmitarrays for unmanned aerial vehicles aided 6G networks," *IEEE Commun. Mag.*, vol. 60, no. 1, pp. 14-20, January 2022.

[7] P.-Y. Feng, S.-W. Qu, and S. Yang, "Octave bandwidth transmitarrays with a flat gain," *IEEE Trans. Antennas Propag.,* vol. 66, no. 10, pp. 5231–5238, Oct. 2018.

[8] B. Rahmati and H. R. Hassani, "High-efficient wideband slot transmitarray antenna," *IEEE Trans. Antennas Propag.*, vol. 63, no. 11, pp. 5149-5155, Nov. 2015.

[9] X.-J. Yi, T. Su, B. Wu, J.-Z. Chen, L. Yang and X. Li, "A double-layer highly efficient and wideband transmitarray antenna," *IEEE Access*, vol. 7, pp. 23285-23290, 2019.
[10] X. Wang, P.-Y. Qin and R. Jin, "Low RCS transmitarray employing phase controllable absorptive frequency-selective transmission elements," *IEEE Trans. Antennas Propag.*, vol. 69, no. 4, pp. 2398-2403, April 2021.
[11] L. Dussopt, A. Moknache, T. Potelon and R. Sauleau, "Switched-beam E-band transmitarray antenna for point-to-point communications," *2017 11th Eur. Conf. Antennas Propag. (EuCAP)*, 2017, pp. 3119-3122.
[12] M. Wang, S. Xu, N. Hu, W. Xie, F. Yang and Z. Chen, "A low-profile wide-angle reconfigurable transmitarray antenna using phase transforming lens with virtual focal source," *IEEE Trans. Antennas Propag.*, doi: 10.1109/TAP.2022.3168648.
[13] L.-Z. Song, P.-Y. Qin, S.-L. Chen and Y. J. Guo, "An elliptical cylindrical shaped transmitarray for wide-angle multibeam applications," *IEEE Trans. Antennas Propag*., vol. 69, no. 10, pp. 7023-7028, Oct. 2021.
[14] J. Hu, H. Wong and L. Ge, "A circularly-polarized multi-beam magneto-electric dipole transmitarray with linearly-polarized feeds for millimeter-wave applications," *IEEE Trans. Antennas Propag*., doi: 10.1109/TAP.2022.3161321.
[15] Y. Hou, L. Chang, Y. Li, Z. Zhang and Z. Feng, "Linear multibeam transmitarray based on the sliding aperture technique," *IEEE Trans. Antennas Propag*., vol. 66, no. 8, pp. 3948-3958, Aug. 2018.
[16] S. H. Zainud-Deen, S. M. Gaber, H. A. Malhet, and K. H. Awadalla, "Cylindrical perforated transmitarrays," *Proc. 2nd Middle East Conf. Antennas Propag.*, Dec. 2012, pp. 1–7.
[17] M. Beccaria, P. Pirinoli and F. Yang, "Preliminary results on conformal transmitarray antennas," *2018 IEEE Antennas Propag. Soc. Int. Symp. USNC/URSI Natl. Radio Sci. Meet. APSURSI*, 2018, pp. 265-266.
[18] T. A. Hill, J. R. Kelly, M. Khalily, and T. W. C. Brown, "Conformal transmitarray for scan loss mitigation with thinned reconfiguration," *Proc. 13th Eur. Conf. Antennas Propag. (EuCAP)*, Mar. 2019, pp. 1–5.
[19] P.-Y. Qin, L.-Z. Song and Y. J. Guo, "Beam steering conformal transmitarray employing ultra-thin triple-layer slot elements," *IEEE Trans. Antennas Propag.*, vol. 67, no. 8, pp. 5390-5398, Aug. 2019.
[20] L.-Z. Song, P.-Y. Qin and Y. J. Guo, "A high-efficiency conformal transmitarray antenna employing dual-layer ultrathin Huygens element," *IEEE Trans. Antennas Propag.*, vol. 69, no. 2, pp. 848-858, Feb. 2021.
[21] L.-Z. Song, P.-Y. Qin, S. Maci and Y. J. Guo, "Ultrawideband conformal transmitarray employing connected slot-bowtie elements," *IEEE Trans. Antennas Propag.*, vol. 69, no. 6, pp. 3273-3283, June 2021.
[22] X. Wang, "Advanced transmitarrays and their beam scanning for future wireless communications," University of Technology Sydney, Sydney, 2021.
[23] L.-Z. Song, "Advanced conformal transmitarrays for 5G and beyond wireless communications," University of Technology Sydney, Sydney, 2021.
[24] L. W. Wu, et. al., "High-transmission ultrathin Huygens' metasurface with 360° phase control by using double-layer transmitarray elements," *Phys. Rev. Appl.* 12(2), 024012 (2019).
[25] M. R. Akram, C. He, and W. Zhu. "Bi-layer metasurface based on Huygens' principle for high gain antenna applications." *Optics Express* 28.11 (2020): 15844-15854.
[26] S. Sakurai, J. G. N. Rahmeier, T. Tomura, J. Hirokawa and S. Gupta, "Millimeter-wave Huygens' transmit arrays based on coupled metallic resonators," *IEEE Trans. Antennas Propag*., vol. 69, no. 5, pp. 2686-2696, May 2021.
[27] X. Wang, P.-Y. Qin, A. T. Le, H. Zhang, R. Jin and Y. J. Guo, "Beam scanning transmitarray employing reconfigurable dual-layer Huygens element," *IEEE Trans. Antennas Propag.*, vol. 70, no. 9, pp. 7491-7500, Sept. 2022.
[28] C. Xue, Q. Lou, and Z. N. Chen, "Broadband double-layered Huygens' metasurface lens antenna for 5G millimeter-wave systems," *IEEE Trans. Antennas Propag.*, vol. 68, no. 3, pp. 1468–1476, 2020.
[29] C. Tian, Y. Jiao, G. Zhao and H. Wang, "A wideband transmitarray using triple-layer elements combined with cross slots and double square rings," *IEEE Antennas Wireless Propag. Lett.*, vol. 16, pp. 1561-1564, 2017.
[30] Q. Luo, S. Gao, M. Sobhy and X. Yang, "Wideband transmitarray with reduced profile," *IEEE Antennas Wireless Propag. Lett.*, vol. 17, no. 3, pp. 450-453, March 2018.
[31] Z. H. Jiang, F. Wu, T. Yue and W. Hong, "Wideband and low-profile integrated dual-circularly-polarized transmit-arrays enabled by antenna-filter-antenna phase shifting cells," *IEEE Trans. Antennas Propag.*, vol. 69, no. 11, pp. 7462-7475, Nov. 2021.
[32] X. Wang, Y. Cheng and Y. Dong, "Millimeter-wave high-efficiency double-layer transmitarray antenna using miniaturized dual-polarized elements," *IEEE Trans. Antennas Propag.*, doi: 10.1109/TAP.2022.3177477.
[33] F. Wu, J. Wang, L. Xiang, W. Hong and K. -M. Luk, "A wideband dual-polarized magneto-electric dipole transmitarray with independent control of polarizations," *IEEE Trans. Antennas Propag*, doi: 10.1109/TAP.2022.3168678.
[34] W. Lin and R. W. Ziolkowski, "Electrically small, low-profile, Huygens circularly polarized antenna," *IEEE Trans. Antennas Propag.*, vol. 66, no. 2, pp. 636-643, Feb. 2018.
[35] W. F. Moulder, "Novel implementations of ultrawideband tightly coupled antenna arrays," Order No. 3535137, The Ohio State University, Ann Arbor, 2012.
[36] https://www.lpkf.com/en/industries-technologies/electronics-manufacturing/3d-mids-with-laser-direct-structuring-lds